Quantum Opt. 5 (1993) 257–273. Printed in the UK

Soliton dragging in discrete and distributed amplifiers

M N Islam†, M Mihailidi‡, C E Soccolich‡, E A deSouza‡,
W Pleibel‡, R H Stolen‡, J R Simpson‡ and D J DiGiovanni‡

† Department of Electrical Engineering and Computer Science, University of Michigan, Ann Arbor, MI 48109, USA
‡ AT&T Bell Laboratories, Holmdel, NJ, 07733, USA

Received 16 March 1993, in final form 3 May 1993

Abstract. We introduce erbium-doped fibre amplifiers (EDFA) into soliton-dragging logic gates (SDLG) to improve their performance in terms of switching energy, fan-out and tolerance to timing jitter. In particular, we experimentally and numerically examine the frequency shifts associated with soliton dragging for orthogonally polarized pulses interacting in discrete and distributed amplifiers. We show that EDFA asymmetrize the interaction between pulses, leading to a frequency shift even when pulses completely walk through each other. The gain can increase the fan-out and/or reduce the switching energy, while proper positioning of the amplifier can loosen the timing restrictions for SDLG. We find reasonable agreement between calculations and measurements in the discrete amplifier case. However, discrepancies for the distributed amplifier case may result from non-uniform gain profiles along the length of the amplifier.

1. Introduction

Recently soliton-dragging logic gates (SDLG) have been shown to satisfy all requirements for a digital optical processor [1]. In soliton dragging, the interaction between two temporally coincident, orthogonally polarized pulses leads to a frequency change and, after propagating in a length of dispersive fibre, into a time shift. For applications to ultrafast switching systems and local and metropolitan area networks, the performance of the soliton logic gates needs to be improved in terms of the switching energy, timing constraints, fan-out and latency or fibre length.

Erbium-doped fibre amplifiers (EDFA) have made significant changes in the long-haul lightwave systems that are currently being designed [2]. Could EDFA also help to improve the performance of SDLG? One option is to place the EDFA before the logic gate, in which case the composite device appears to have lower switching energy and higher fan-out. However, a more clever approach is to imbed the EDFA into the soliton logic gate and have the amplification to be a part of the soliton dragging mechanisms, in which case we can lower the switching energy, increase the fan-out and relax the timing constraints [3]. To understand the role of EDFA in soliton dragging, we must study the frequency shifts associated with soliton dragging in amplifiers.

In this paper we investigate both experimentally and numerically the interaction between orthogonally polarized pulses in discrete and distributed amplifiers. The characteristic length for a soliton is known as the soliton period Z_0, which is the length over which a soliton experiences significant changes from group-velocity dispersion

0954-8998/93/050257+17 $7.50

and/or the non-linearity in the fibre. By discrete gain we mean an EDFA whose length is short compared to Z_0, and by a distributed gain we mean an EDFA whose length is comparable or longer than Z_0. We show that the amplifier asymmetrizes the interaction between the two orthogonally polarized pulses, leading to a frequency chirp even when the two pulses completely walk through each other. We also show that proper positioning of the amplifier can loosen the timing constraints of soliton dragging.

In the next section we review the SDLG and chirp mechanisms in soliton dragging. Then, in section 3 we describe the experimental apparatus and the specially designed EDFA used. The experimental results in short, highly-doped EDFA and long, lightly-doped EDFA are presented in section 4, and we confirm the observed behavior using numerical simulations in section 5. Finally, in section 6 we discuss implications for soliton switching devices and short pulse propagation in transmission systems.

2. Chirp mechanisms in soliton dragging

SDLG are one example of a more general architecture of devices that we call time-domain chirp switches. As shown in figure 1(a), a time-domain chirp switch consists of a non-linear chirper followed by a dispersive delay line and has two orthogonally polarized inputs (signal and control pulses). In the absence of a signal pulse, the control pulse propagates through both sections and arrives at the output within the clock window. For a cascadable switch, the self-induced chirps on the control in both sections must balance, and the output pulse must resemble the input. Adding the signal pulse creates a time-varying index change that chirps the control pulse and shifts its centre frequency. As the chirped control pulse propagates through the soliton-

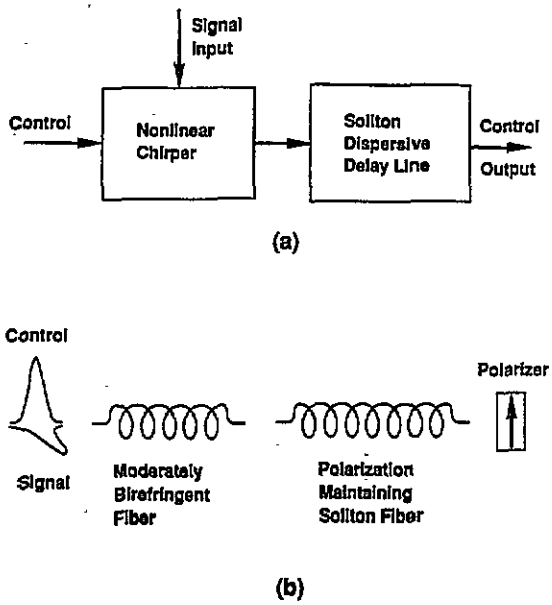

Figure 1. (a) General architecture for an all-optical time-domain chirp switch (TDCS). The signal creates a time-varying index change in the non-linear chirper, and the soliton dispersive delay line translates the frequency shift into a time shift. (b) A soliton-dragging logic element is an all-fibre example of a TDCS.

dispersive delay line, the frequency shift is translated into a time change. For proper switching, the frequency shift must lead to at least a two or three pulse width shift, but the maximum shift must be less than half of the separation between adjacent bits. In a SDLG the non-linear chirper corresponds to a moderately birefringent fibre, and the soliton-dispersive delay line corresponds to a long polarization-maintaining fibre (figure 1(b)). In this paper we will focus on the frequency changes after the non-linear chirper, and we will introduce EDFA within the moderately birefringent fibre that acts as the non-linear chirper.

We study next the soliton dragging mechanisms and techniques for expanding the acceptable timing window for SDLG. We begin by providing an intuitive picture of cross-phase modulation and walk-off [5] that results in a shift of the frequency centroid $\Delta\omega_c$ of the control pulse. The formulae from which figure 2 is derived are given in [3], where pulse shape changes that may be due to dispersion are neglected.

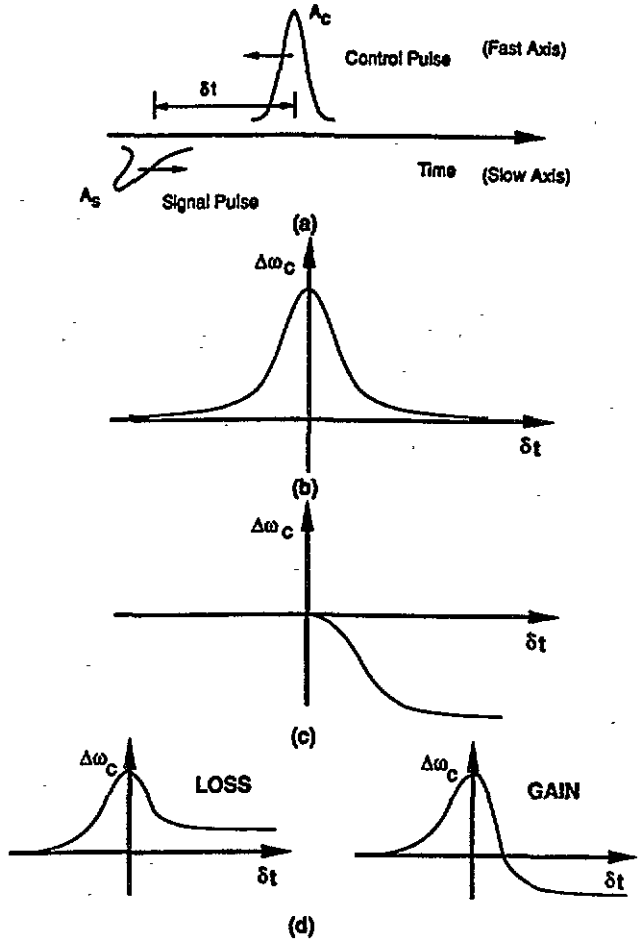

Figure 2. (a) Interaction between orthogonally polarized control and signal pulses. Schematic plot of the shift in the control pulse centre frequency $\Delta\omega_c$ plotted against the pulse separation δt for: (b) complete walk-through of the two pulses; (c) when the two pulses temporally coincide at the input; and, (d) with discrete loss or gain when the two pulses coincide.

The group velocity dispersion in the fibre translates the frequency shift into a timing shift ΔT.

Consider the interaction between a control pulse (amplitude A_c) along the fast axis and a signal pulse (A_s) along the slow axis (figure 2(a)). We plot the shift in the control pulse centre frequency $\Delta\omega_c$ versus the initial pulse separation δt as the two pulses walk-off. For a complete walk through of two pulses whose shapes remain constant during the interaction the collision is almost completely elastic. As shown in figure 2(b), the frequency shift curve is symmetric and after the collision the centre frequency returns to its original value. There is a slight shift in the time and phase of the control pulse because of the temporary frequency shift; but, in general, the resulting time shift is only a small fraction of a pulse width.

In SDLG the two pulses start coincident and then walk-off. Thus, each pulse experiences only part of the complete collision and a substantial net frequency shift results (figure 2(c)). A control pulse along the fast axis slows down and we can obtain a time shift of several pulse widths. Typically the two pulses must be synchronized to within a pulse width to guarantee sufficient time shift from soliton dragging, and this is the origin of the timing restrictions for soliton dragging.

Introducing loss or gain can asymmetrize the interaction during the walk-off. Consider a complete walk through of the pulses when the optical fibre has an abrupt loss or gain at the point where the two pulses maximally overlap. The control pulse still speeds up in the first half and slows down in the second half. However, since the rate of change of the control frequency is proportional to the signal intensity, there will be a net frequency increase (speed up) with loss and a net frequency decrease (slow down) with gain (figure 2(d)). From this intuitive picture we see that to relax the timing restrictions we must allow for almost complete walk-through of the two pulses while somehow asymmetrizing the interaction. Therefore, we expect that introducing an EDFA during the collision between the control and signal pulses will widen the timing restrictions.

3. Experimental apparatus and fibre characteristics

To test the effect of amplification on soliton dragging, we use the apparatus of figure 3(a). The laser source (figure 3(b)) is a Tl:KCl colour centre laser that is passively mode-locked using an InGaAsP saturable absorber [6, 7]. The typical output from the laser is nearly transform-limited pulses of 500 fs duration (spectral width $\Delta\lambda$ of approximately 8 nm) with pulse energies of 600 pJ and a centre wavelength between 1.53 and 1.56 μm. The laser wavelength is tuned by rotation of a 2 mm thick quartz birefringent tuning plate. The colour centre laser is pumped by a CW Nd:YAG laser, and the gain crystal is kept at cryogenic temperatures under vacuum in a Dewar.

After passing through an isolator, the laser beam is divided between a control and signal arm, and the ratio of power can be varied by rotation of a half-wave plate. A stepper-motor controlled delay stage varies the timing between the two arms. The signal corresponds to the first-order beam from an acousto-optic modulator, which shifts the signal beam by 80 MHz from the control arm. Although the slight frequency shift does not change the pulse walk-off, the interaction between the optical and acoustic wave guarantees a random phase between the control and signal pulses and any phase-dependent interference averages to zero. The two arms are then combined using a polarizing beam splitter, and the collinear beams are coupled into the fibre.

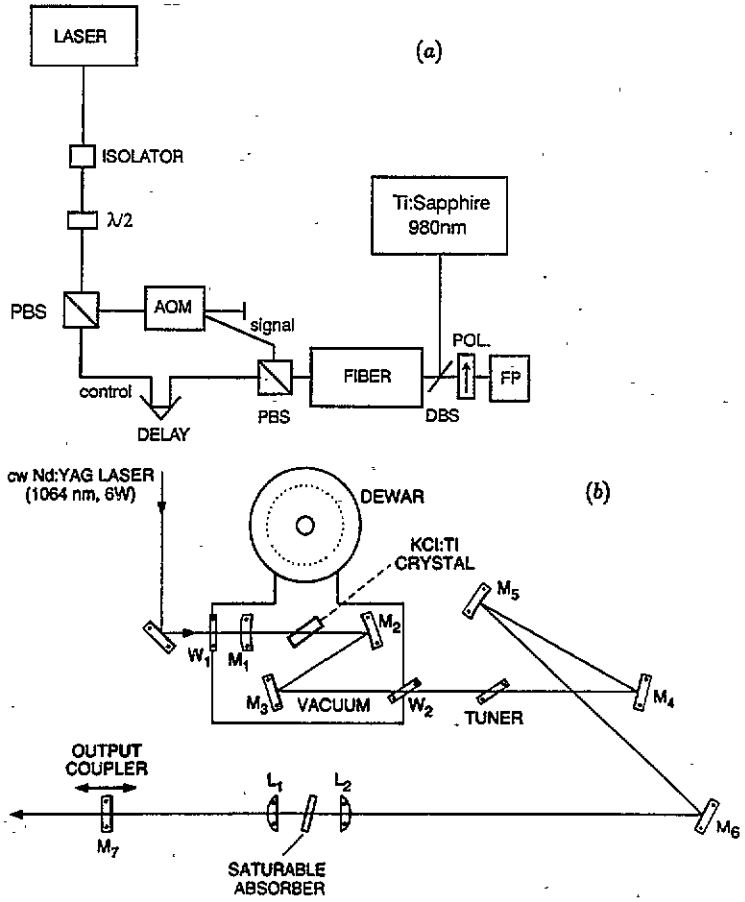

Figure 3. (a) Experimental apparatus for testing soliton-dragging in discrete and distributed amplifiers (PBS, polarizing beam splitter; DBS dichroic beam splitter; POL, polarizer; FP, Fabry–Perot interferometer; AOM, acousto-optic modulator). (b) The laser source is a passively mode-locked Tl:KCl colour centre laser (M, mirrors; L, lenses; W, window).

The fibre is pumped from the back side by a Ti:sapphire laser through a dichroic beam splitter, which reflects the 0.98 μm pump while passing both polarizations of 1.55 μm light. The output end of the fibre is polished to a 7° bevel to prevent lasing within the amplifier. We handle each of the fibres carefully to maintain the polarization axes, and the polarization extinction was better than 15 dB after even the spliced fibres (see below). At the fibre output a polarizer is oriented along the control axis, and the output spectrum is monitored using a Fabry–Perot interferometer.

For the discrete gain measurements, we use a 1.7 m length of highly-doped EDFA spliced betwen two lengths of identical moderately birefringent fibre. The axes are monitored while splicing the fibres, and a maximum loss of 0.7 dB is incurred at each splice. The length of the input moderately birefrigent fibre is between 11 and 30 m, while the length of the output fibre is 31 m. These undoped fibres have a birefringence of approximately $\Delta n \approx 2.2 \times 10^{-5}$, a zero dispersion wavelength of around 1.5 μm, and a group-velocity dispersion of about 2.5 ps nm^{-1} km^{-1} at 1.54 μm. For 500 fs pulses the soliton period is 40 m and the walk-off length ($L_{wo} = c\tau/\Delta n$) is about 7m. The 1.7m

EDFA has a doping level of approximately 1660 ppm, a core-cladding index difference of 0.0204, a single-mode cut-off wavelength of 1.41 μm and a zero dispersion wavelength of approximately 1.49 μm. The core size of the fibre is chosen to guarantee both single spatial mode and operation in the soliton or anomalous group velocity dispersion regime. Furthermore, the fibre preform is squashed before pulling in a ratio of 4:3 to introduce a measured birefringence of 3.6×10^{-5} in the EDFA, which means that the polarizations can be maintained in the fibre.

The distributed gain measurements are performed in a single 25 m length of lightly doped EDFA. The doping level is approximately 165 ppm and the core-cladding index difference is 0.021. The fibre preform is squashed to a ratio of 5:4 between the two axes, and the core size is chosen to obtain measured values of cut-off at 1.42 μm, zero dispersion wavelength of 1.51 μm, and a birefringence of 2.9×10^{-5}. For 640 fs pulses at 1.54 μm the soliton period is about 53 m and the walk-off length is 6.6 m. Since the EDFA is more than two walk-off lengths long, pulses coinciding at the beginning of the amplifier can fully interact within the EDFA. However, since the amplifier is only about half of a soliton period, we might not expect drastic pulse shape changes except at high gain levels.

4. Experimentally measured frequency shifts

As mentioned earlier, we concentrate here on the frequency shifts at the end of the non-linear chirper in figure 1(a). To make a SDLG, we would add a polarization-maintaining fibre afterwards to convert the frequency change into a timing shift. We plot the frequency shift of the control pulse normalized to the input spectral width of the pulse versus the temporal separation between the control and signal pulses at the input of the fibre normalized to the input pulse width. Zero time delay corresponds to the pulses coinciding at the fibre input.

One serious complication in performing the experiments is that the EDFA is not a linear amplifier at the power levels used in the experiment. That is, the gain for the control pulse decreases in the partially saturated amplifier when the signal pulse is added. We compensate for the amplifier saturation by referencing the frequency shift of the control to a background control pulse spectrum measured when the control and signal are separated by many pulse widths. Since the EDFA has very long lifetimes (0.1–1 ms), much longer than the 12 ns separation between pulses from the laser, the decrease in gain associated with saturation will be independent of the pulse separation. To illustrate the spectral shift data, we include in figure 4 a photograph of the spectral output from the Fabry–Perot when two pulses coincide at the input. The centred spectrum corresponds to the stored spectrum from when the two pulses are separated by many pulse widths, and we find that the spectrum shifts to the right due to soliton dragging. In the following data curves we plot only the shift of the spectrum normalized to the input spectral width.

4.1. Experiments in discrete amplifiers

In figure 5 we plot spectral shift data for the discrete amplifier case with different gain levels, which are changed by varying the pump power. Figure 5(a) uses a 30 m length of the input moderately birefringent fibre, and then this fibre is cut back to 15 m (figure 5(b)) and finally 11 m (figure 5(c)), where the final length corresponds to about

1.6 walk-off lengths. In figure 5(a) there are three features; the feature around zero delay corresponds to collision at the fibre input, the feature near 4 pulse widths corresponds to collision in the amplifier, and the feature near 8 pulse widths corresponds to collision at the fibre output. In these experiments the input signal and control energies are kept fixed around 2 pJ per pulse and the output energy varies between 2.5 pJ and 10 pJ.

If we adjust to near unity gain (i.e. as if no amplifier), then we only have features at the beginning and end of the fibre (cf the lowest gain case in figures 5(a) or (c)). As we can see from figure 2, at the beginning we see one half of the collision, and at the end of the fibre we see the other half of the collision (i.e., at the fibre input the pulses start coincident, while at the fibre output the pulses finish coincident). Therefore, the magnitude of the shifts should be comparable, but the sign of the shift should be opposite from the beginning to the end of the fibre.

As the gain is increased from unity, we observe an additional frequency shift when the pulses collide within the amplifier. The feature centred at zero delay does not change because it precedes the amplifier. Since the frequency shift is proportional to the signal intensity, after amplification the frequency shift at the fibre end is larger than at the input. The features after the amplifier increase in proportion to gain minus one. Thus, the amplifier has two effects: to introduce additional shifts due to asymmetric interactions within the amplifier and to asymmetrize the shift between the beginning and end of the fibre.

By cutting back the length of the first moderately birefringent fibre, the position of the amplifier measured in units of walk-off length moves closer to the fibre input, and the left two features in figure 5 move closer to each other. For example, in figure 5(b) we find the two frequency features are adjacent, and in figure 5(c) they merge to form a broadened frequency shift. The broadened frequency shift of figure 5(c) is desired to increase the tolerance to timing jitter in a SDLG.

If we increased the length of the second moderately birefringent fibre, then the position of the rightmost frequency feature would shift to longer times. In fact, in a SDLG we typically would use a 350 m to 500 m length of fibre in the final section. We can approximate the case of a very long second moderately birefringent fibre by

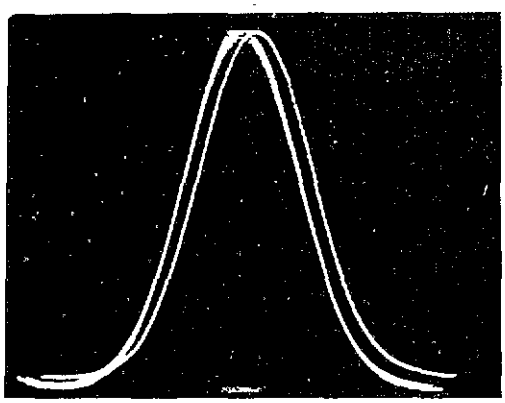

Figure 4. Copy of the spectral output from the Fabry–Perot for different separations between the control and signal pulses. The Fabry–Perot has close mirror spacing ($< 10\,\mu m$) so the free spectral range is larger than the pulse spectral width. The centred curve is stored when the two pulses are separated by many pulse widths, while the shifted curve corresponds to pulses coinciding at the fibre input.

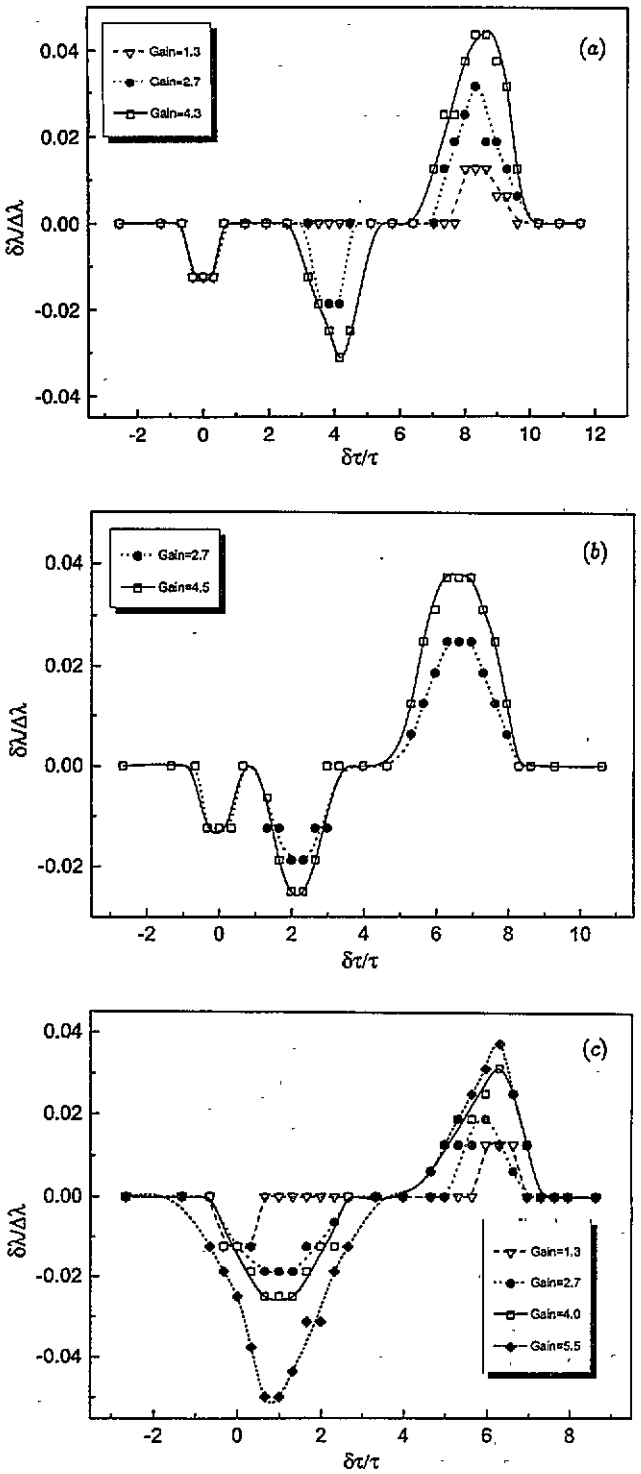

Figure 5. Normalized spectral shift data plotted against separation between the control and signal pulses at the fibre input for the discrete amplifier case and different gain levels. The output fibre is 31 m long, the EDFA is 1.7 m long and the input fibre is varied in length between (a) 30 m, (b) 15 m and (c) 11 m (MBF moderately birefringent fibre).

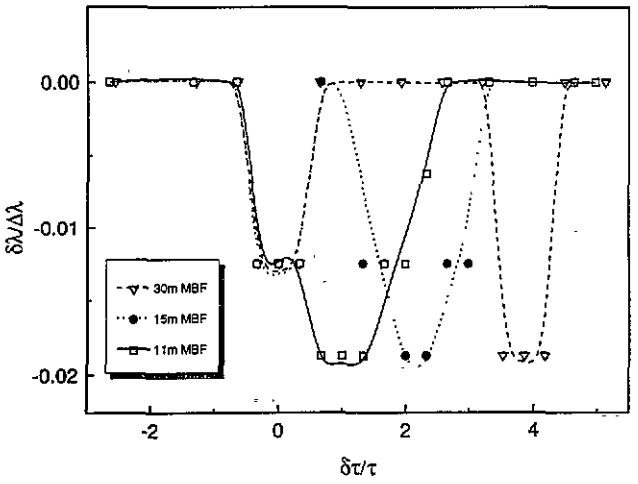

Figure 6. Data from figure 5 for a gain of 2.7 and assuming that the final fibre end is many walk-off lengths away. Depending on the position of the discrete amplifier, the timing window for soliton-dragging can be broadened or additional windows can be created.

ignoring the rightmost features in figure 5. For example, in figure 6 we extract from figure 5 the frequency shift for different lengths of the first fibre at a gain of approximately 2.7. We see that the window of positions over which pulse interactions lead to a frequency shift can be broadened or supplemented by introducing a discrete EDFA within the interaction region.

4.2. Experiments in distributed amplifiers

In the next set of experiments we use a 25 m length of 160 ppm EDFA that is moderately birefringent. Figure 7 shows the frequency shift when the input energy is held fixed at 1.5 pJ and the gain is varied, while figure 8 shows the frequency shift when the output energy is held fixed at 9.3 pJ and the input and gain levels are varied. Once again, we find three frequency features corresponding to collisions at the beginning and end of the fibres as well as somewhere in the amplifier. The behaviour in figure 7 is similar to figure 5 in that changing the gain does not affect the leftmost feature, but it increases the two right features. In figure 7 for the case of distributed amplifier with fixed input, we also find that increasing the gain tends to shift the second feature closer to the beginning of the fibre while broadening out the two right features. On the other hand, if the output is held fixed, then increasing the gain decreases the input amplitude and, hence, the shift at the beginning of the fibre. Therefore, in figure 8 increasing the gain decreases the leftmost feature, which is proportional to the input intensity, while it still increases the second and third features.

We have experimentally observed the pulse width dependence upon launched power after propagating through long fibre lengths and determined empirically the fundamental soliton energy to be approximately 4 pJ. Therefore, working at higher gain levels where the powers exceed approximately 9 pJ results in formation of higher order solitons. Higher-order solitons result in generation of additional frequency components and pulse narrowing, which can enhance frequency shifts associated with

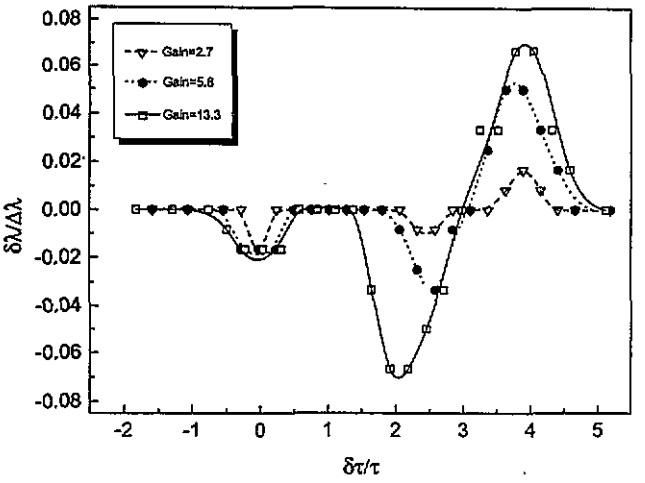

Figure 7. Normalized spectral shift data plotted against separation between the control and signal pulses at the fibre input for the distributed amplifier case. The input energy is fixed at 1.5 pJ, and the gain is varied by changing the pump power. The EDFA is 25 m long, which corresponds to about four walk-off lengths.

Raman effects. These distortions at higher powers limit our abilty to resolve small frequency shifts.

Figures 7 and 5(b) show qualitatively similar behaviour, although the position of the rightmost feature is further out in figure 5(b) since the fibre ends later. The amplitude of the shifts differ slightly, but that may be because of differences between the fibres and may be within the uncertainty of the gain level measurements. The frequency features are more asymmetric in the distributed gain case, which may reflect slight changes in the pulse shape as the soliton propagates. One reason for the similarity in the figures may be because the distributed amplifier is still only about a half of a soliton period long, so the soliton does not have much of an opportunity to readjust its shape within the amplifier except at high gain levels. However, the

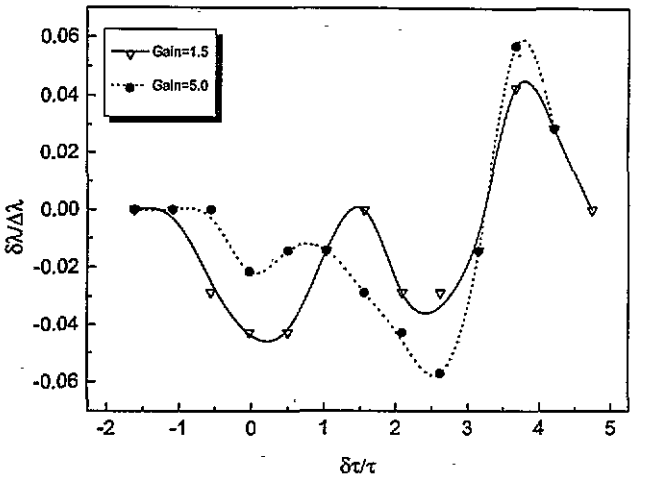

Figure 8. Normalized wavelength shift for the distributed amplifier case as in figure 7, except the output energy is held fixed at 9.3 pJ and the input and gain levels are varied.

distributed gain case is easier to implement since it does not require splices and matching the fibre axes.

5. Numerical simulations to verify results

To verify the experimentally observed behaviour, we also numerically solved the couped non-linear Schrödinger equation. In a linearly birefringent fibre, the coupled non-linear Schrödinger equation can be written as [4]

$$-\mathrm{i}\left(\frac{\partial u}{\partial z}+\delta\frac{\partial u}{\partial t}\right)=\frac{1}{2}\frac{\partial^2 u}{\partial t^2}+|u|^2u+\frac{2}{3}|v|^2u-\mathrm{i}\gamma u$$

$$-\mathrm{i}\left(\frac{\partial v}{\partial z}-\delta\frac{\partial v}{\partial t}\right)=\frac{1}{2}\frac{\partial^2 v}{\partial t^2}+|v|^2v+\frac{2}{3}|u|^2v-\mathrm{i}\gamma v \tag{1}$$

where we have used the standard soliton normalizations. The propagation operator on the left-hand side includes the effect of birefringence, and the terms on the right-hand side correspond from left to right to group-velocity dispersion, self-phase modulation, cross-phase modulation and gain. The lengths are normalized to z_c, the times are normalized to t_c and the powers to P_c, where

$$\frac{t_c^2}{z_c}=\frac{\lambda^2 D}{2\pi c} \qquad \text{and} \qquad P_c z_c=\frac{\lambda A_{\text{eff}}}{2\pi n_2}. \tag{2}$$

In particular, the amplitudes u, v scale as $(P/P_c)^{1/2}$ and the soliton period is given by $Z_0=\frac{1}{2}\pi Z_c$ or $Z_0=0.322(\pi^2c/\lambda^2)(\tau^2/|D|)$. Furthermore, the normalized birefringence is given by $\delta=\pi\Delta n(\tau/1.763)/\lambda^2|D|$. We use a split-step Fourier transform technique to solve equation (1), and we study the shift of the control frequency centroid, which is defined by

$$\omega_c''(z)=\int_{-\infty}^{\infty}\mathrm{d}\omega\omega|u(\omega,z)|^2\left(\int_{-\infty}^{\infty}\mathrm{d}\omega|u(\omega,z)|^2\right)^{-1}. \tag{3}$$

To simulate the discrete amplifier case, we solve equation (1) for the soliton propagation and introduce an abrupt gain at the appropriate position. At the amplifier location we just increase the amplitudes along both axes and ignore any pulse shape changes or any readjustments of the relative pole positions due to the birefringence in the amplifier. In figure 9 we show exemplary simulations for an intensity gain of 2.7, $u=v=0.45$ at the input, and a normalized birefringence of $\delta=3.28$. The length of the fibre after the amplifier is $L_2=0.765Z_0$, and the length of the first fibre is varied between 0.27 and $0.69Z_0$.

The corresponding experimental data (extracted from figure 5) are also included with the simulations, and we find reasonable agreement between simulations and experiments for the discrete gain case. One reason the experimental features appear narrower is that it is difficult to resolve frequency shifts under 1% because of laser amplitude fluctuations, so in many cases we set shifts below our resolution simply to zero. This is also why the experimental curves have flat sections (i.e., set to zero because below our resolution) whereas the simulations do not exhibit plateaus. Nonetheless, as the length of the first fibre is reduced, the two leftmost features move

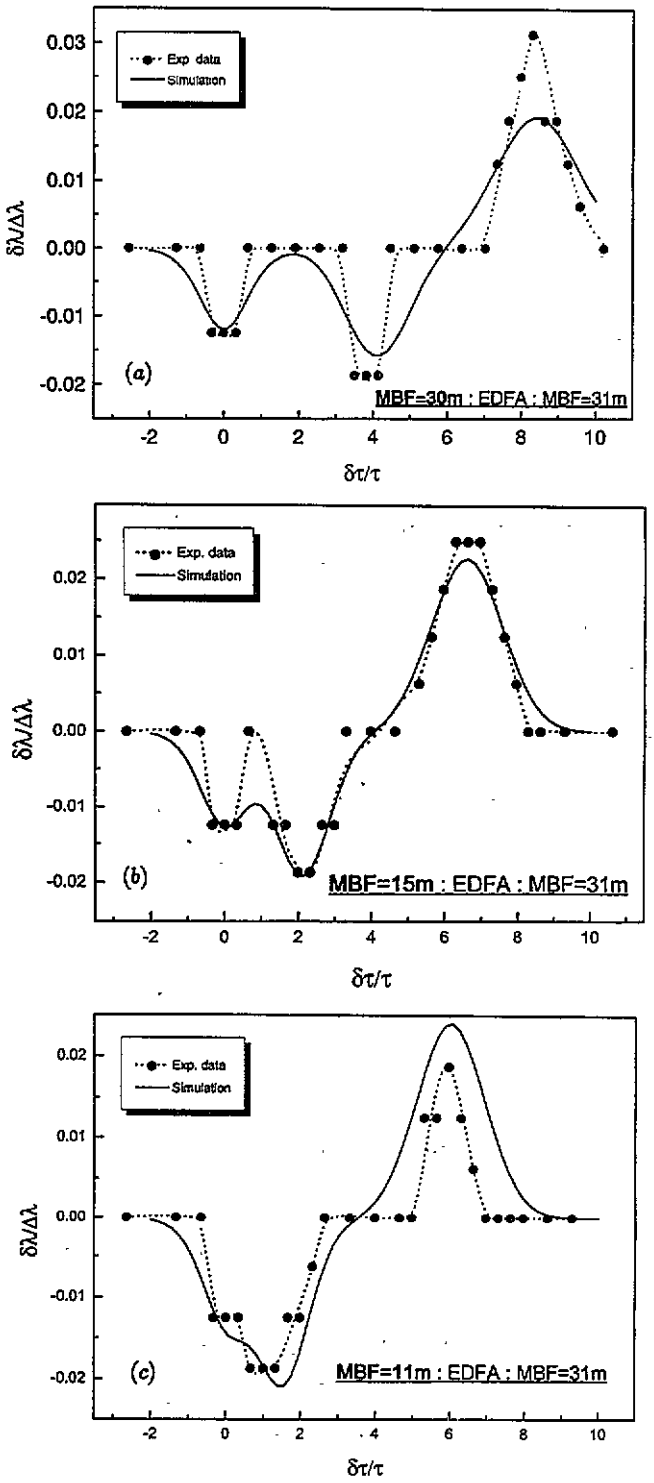

Figure 9. Simulations of the wavelength shift versus input pulse separation for the discrete amplifier case with a gain of 2.7 and the input fibre length varied: (a) 30 m; (b) 15 m and (c) 11 m. The experimental data are extracted from the corresponding curves in figure 5.

closer and coalesce. Since the soliton pulses propagate a longer distance before amplification in figure 9(a), and since the solitons broaden while propagating at low intensities, we find the two rightmost frequency features are broader in figures 9(a) than in the shorter fibre cases of figures 9(b) and (c). The experimental shifts in the short fibre case of figure 9(c) undershoot simulations and in the long fibre case of figure 9(a) overshoot the simulations. This may be due to pulse shape changes associated with a slight chirp on the pulses launched from the colour centre laser, which is ignored by the simulations that assume secant hyperbolic inputs. Another clue supporting this hypothesis is that the discrepancy grows as the pulse propagates farther down the fibre. Note that the discrepancy is within the 1% frequency shift resolution already mentioned.

5.1. Simulations of the distributed amplifier case

In the distributed amplifier case, we find that the soliton can reshape itself during the amplification. Once again we solve equation (1), but now we assume a single length of fibre and we introduce the gain terms throughout the propagation. As a simple approximation, we asume uniform gain throughout the fibre, which means that the net energy gain is

$$G=\frac{E_{\text{out}}}{E_{\text{in}}}=\exp(2\gamma z) \tag{4}$$

where γ is the uniform gain coefficient and E stands for energy.

In figure 10 we show simulations corresponding to the experimental results displayed in figure 7. The gain is varied between 2.7 and 13.3, $u=v=0.59$ at the input, the normalized birefringence is $\delta=4.5$ and the fibre length is $L=0.47Z_0$. The experimental data for each of the cases (from figure 7) are overlayed with the simulations in figure 10. The notable difference between simulation and experiment is that the experimental dip toward zero around $\delta\tau/\tau=1$ to 1.5 is much more pronounced than found in the simulations. Another difference is the magnitude of the frequency shift at the fibre end, where simulations consistently overshoot the experimental values. Nonetheless, the simulation confirms three frequency features, just as we saw in the discrete gain case.

We plot in figure 11 a series of simulations for gain varying from 1 to 13.3 in the distributed amplifier. As the gain is increased, the feature centred around $\delta\tau/\tau=2$ increases as well as the feature from the fibres end. Comparing figure 11 with the data of figure 7, we observe several differences. As in the discrete gain case, the experimental curves appear narrower, but that may again be due to our resolution in measuring small shifts. Also, the data clearly dips toward zero shift around $\delta\tau/\tau=1$, while the simulation does not show such a sharp feature. There may be several reasons for the discrepancy between theory and experiment in the distributed gain case. First, as in the discrete gain case, the input pulse may have a slight chirp from the laser, so the propagation is different than for a hyperbolic secant pulse shape. Second, there may be some additional non-linear effects arising from soliton self-frequency shifts, particularly at the higher gain levels.

The more serious unknown may be the profile of the gain along the length of the fibre. In the simulations thus far we have assumed a uniform gain profile, but we have not done any cut-back experiments to confirm this assumption. The gain profile will affect the shape of the frequency shift. The most obvious complication is that the

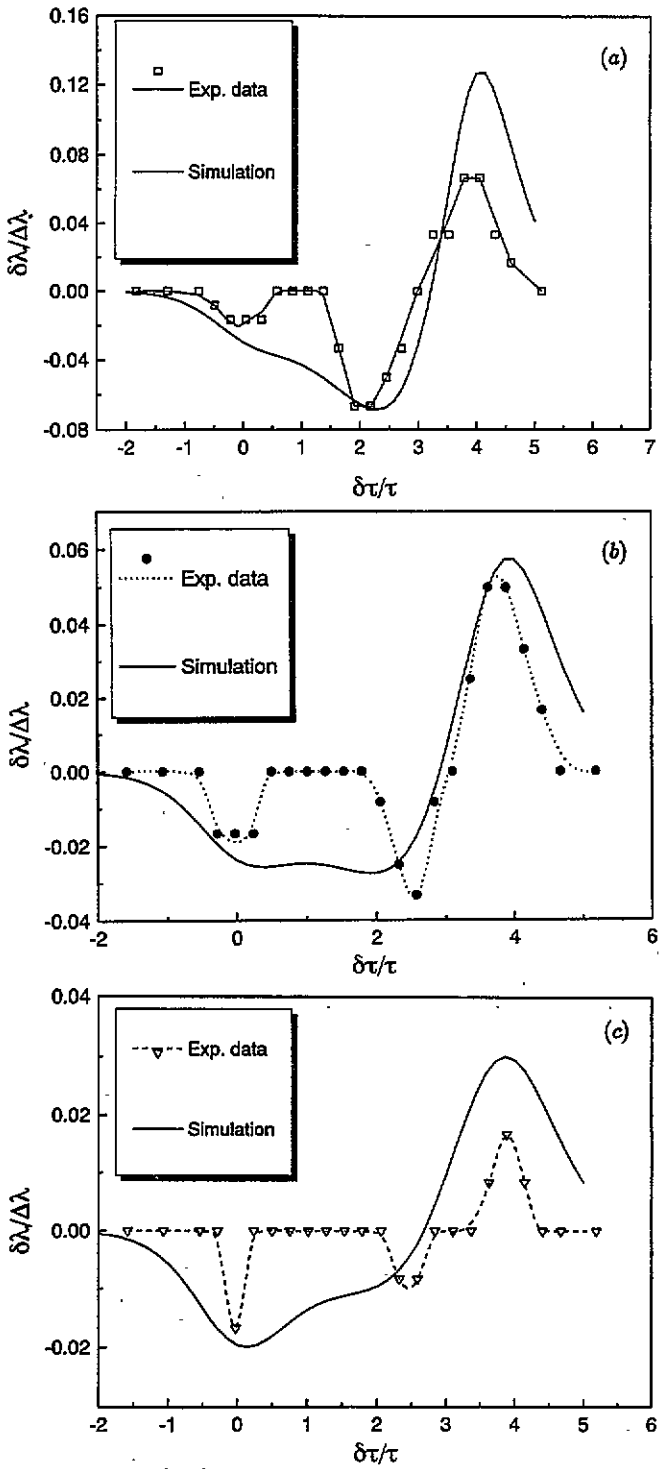

Figure 10. Simulations of the wavelength shift plotted against input pulse separation for the distributed amplifier case with a 25 m EDFA and the gain varied: (a) gain = 13.3; (b) gain = 5.8 and (c) gain = 2.7. The experimental data are extracted from the corresponding curves in figure 7, and the gain is assumed to be uniform along the fibre length.

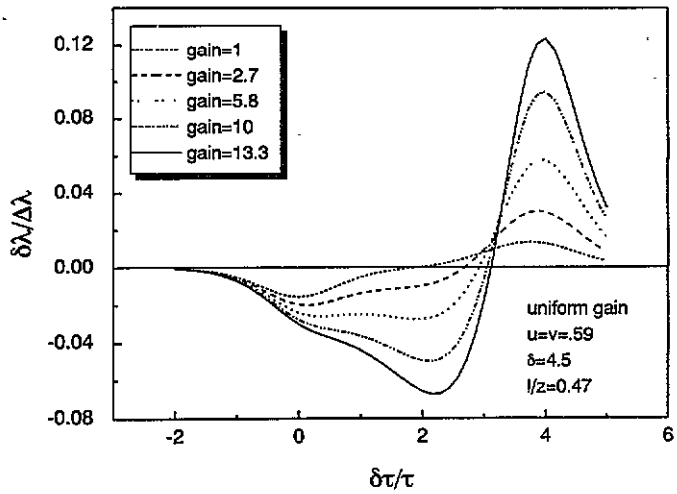

Figure 11. Simulations of the wavelength shift plotted against input pulse separation for a uniform gain in the distributed amplifier and different gain levels.

pump intensity decreases in the 25 m EDFA due to erbium absorption. Another possibility is that the gain profile may actually change with the level of pump power, since the erbium ions in the back end of the fibre may be fully inverted. This would mean that the gain model would have to be different between the high and low gain cases.

As a first-order approximation, we assume that the pump power and gain decrease exponentially starting from the back end of the fibre, i.e. we approximate the gain function in equation (1) as

$$\gamma(z) = \gamma_0 \exp[\kappa(z - L)]. \tag{5}$$

Let G be the net energy gain and define the number of gain lengths L_g as the amount the gain coefficient and pump power decreases by in the fibre (the gain coefficient is $\exp(-L_g)$ of its value at the end of the fibre). Then we find that

$$\gamma_0 = \kappa \ln(G)/2(1 - e^{-\kappa L}) \qquad \kappa = L_g\left(\frac{2}{\pi}\right)\left(\frac{Z_0}{L}\right) \tag{6}$$

where the lengths are given normalized in soliton units. For example, in figure 12 we plot the frequency shift for $u = v = 0.59$ at the input and a gain of 5.8 for different gain attenuation lengths within the 25 m EDFA. As the number of gain lengths increases, all three frequency features decrease in magnitude, but the ratios of the features change.

6. Discussion

We have presented numerical and experimental data to confirm that the collision between orthogonally polarized pulses can lead to frequency shifts, and these frequency shifts are affected by the presence of gain. Gain during the collision asymmetrizes the interaction, thereby leading to a net frequency shift even when pulses completely walk through each other. In the experiments we use specially crafted EDFA that are designed to be single-mode with anomalous group-velocity

dispersion and that are squashed in the preform stage to introduce the proper amount of birefringence. In the discrete amplifier case the EDFA is about $0.25L_{wo}$ and less than 0.035 soliton periods long. On the other hand, in the distributed amplifier the EDFA is about $4L_{wo}$ and about a half of a soliton period long. We find reasonable agreement between simulations and experiments for the discrete gain case, but the discrepancy grows in the distributed gain case.

In long-haul fibre transmission systems being studied currently, approximately 30 m long EDFA are used with pulses over 10 ps in width, which means that the soliton period is many kilometres long. Therefore, these systems are always in the discrete gain limit. However, if sub-picosecond pulses are propagated over the same fibre link, then the soliton period approaches the amplifier length, and we could shift to the distributed amplifier case. Therefore, as the bit rate on time-division multiplexed systems increases and the pulses become shorter, we will begin to shift between the two limits studied in this paper. In particular, as the gain becomes more distributed on the scale of a soliton period, solitons can begin to reshape adiabatically within the amplifier in response to the gain.

The frequency shifts studied here have implications both for soliton transmission systems and soliton-dragging logic gates. For transmission systems where timing errors can lead to increased bit-error rates, collisions between orthogonally polarized solitons in amplifiers can result in frequency and time changes. Similar deleterious effects have been observed when solitons of different frequency collide in amplifiers or when two soliton data trains are launched simultaneously [8]. However, it is precisely these frequency shifts that are exploited to obtain the time shifts required for soliton dragging [3].

As described in section 2, to reduce the sensitivity of SDLG to timing jitter, we want to increase controllably the timing window over which interactions between orthogonally polarized pulses results in frequency changes. This timing window can be increased to at most half of the bit period or spacing between adjacent bits. In the case of the discrete amplifier, we found in figure 5(c) that the timing window at the fibre

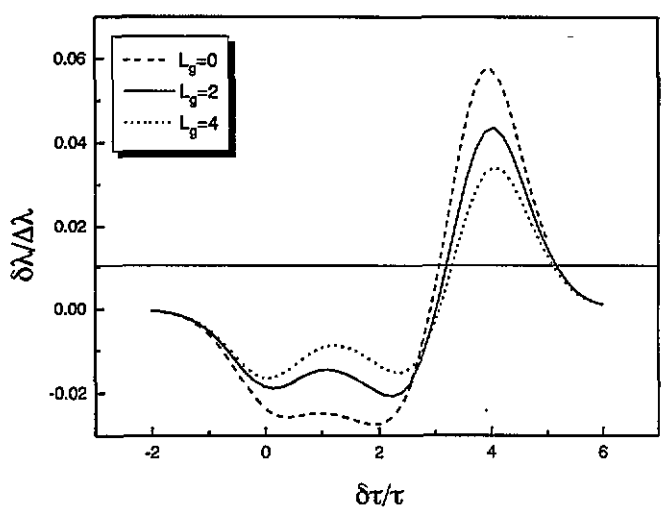

Figure 12. Calculated wavelength shift plotted against initial pulse separation assuming an exponentially varying gain profile in the distributed amplifier case. The gain function and gain lengths are defined by equations (5) and (6), and the net gain is held fixed at 5.8.

input could be broadened by introducing the amplifier at an appropriate location. Since in a SDLG usually we splice to the end a 300 to 500 m long fibre as the soliton dispersive delay line, the frequency shift from the fibre end will be pushed out much further, thus leading to a frequency shift curve more like figure 6. In a similar way, the timing window can also be increased by using a distributed amplifier. Despite the simplicity of having a single distributed amplifier, as this point our inability to predict accurately the experimental behaviour may be one reason to shy away from this approach.

Our experiments show that introducing EDFA into SDLG raise several complications. First, the operation of the device is restricted to the erbium-gain band around 1.53–1.56 μm, and a pump source either at 0.98 or 1.48 μm is required. Second, the amplified spontaneous emission from the amplifier adds noise as well as perhaps other non-linear effects such as the Gordon–Haus effect [9]: we have not evaluated the influence of the Gordon–Haus effect on soliton dragging. Futhermore, there is some uncertainty in assigning gain level to the experiments for the two polarizations because of the amplified spontaneous emission. Since we are using short pulses with broad spectral widths, there is no simple way of filtering the amplified spontaneous emission.

We remain perplexed by the gain profile in the distributed amplifier and its impactkon soliton propagation in the amplifier. The discrepancy in the trend for different gain levels suggests that the gain profile changes with pump power level. In fact, there is experimental evidence showing that the spectral profile of the gain changes with the degree of inversion in the EDFA [10]. A constructive approach might be to turn the problem around and try to find a gain profile in the simulations that will lead to the observed behaviour. If successful, then the frequency shift technique using short pulses can serve as a non-invasive diagnostic tool for mapping out the gain profile.

References

[1] Islam M N 1990 *Opt. Lett.* **15** 417
Islam M N, Soccolich C E and Miller D A B 1991 *Opt. Lett.* **16** 566
[2] Mollenauer L F, Gordon J P and Evangelides S G 1991 *Laser Focus World* Nov. 159–70
[3] Islam M N, Menyuk C R, Chen C-J and Soccolich C E 1991 *Opt. Lett.* **16** 214
[4] Islam M N 1992 *Ultrafast Fiber Switching Devices and Systems* (Cambridge: Cambridge University Press)
[5] Islam M N, Mollenauer L F, Stolen R H, Simpson J R and Shang H T 1987 *Opt. Lett.* **12** 625
[6] Soccolich C E, Islam M N, Mollmann K, Gellerman W and German K R 1992 *Appl. Phys. Lett.* **61** 886
[7] Mollmann K, Gellerman W, Soccolich C E and Islam M N 1993 *Opt. Lett.* **18** 42
[8] Andrekson P A, Olsson N A, Simpson J R, Tanbun-Ek T, Logan R A, Becker P C and Wecht K W 1990 *Electron. Lett.* **26** 1499
[9] Gordon J P and Haus H A 1986 *Opt. Lett.* **11** 665
[10] Simpson J R, Shang H-T, Mollenauer L F, Olsson N A, Becker P C, Kranz K S, Lemaire P J and Neubelt M J 1991 *J. Lightwave Technol.* **9** 228